2017 IEEE International Conference on Systems, Man, and Cybernetics (SMC)
Banff Center, Banff, Canada, October 5-8, 2017

Study on the Force Myography Sensors Placement for Robust Hand Force Estimation

Maram Sakr, Carlo Menon *IEEE Member*

***Abstract*— Force Myography (FMG) is a method of tracking functional motor activity using volumetric changes associated with muscle function. With comparable accuracy and multiple advantages over traditional methods of functional motor activity tracking, FMG has shown a promising potential in terms of applications in human-machine interfaces, tele-operation and healthcare devices. This paper provides a study that explores the effect of the spatial coverage and placement of the Force Myography (FMG) measurements on the accuracy and predictability of the machine learning models of isometric hand force. Five participants were recruited in this study and were asked to exert isometric force along three perpendicular axes while wearing custom built FMG devices. During the tests, the isometric force was measured using a 6 degree-of-freedom (DOF) load cell whereas the FMG signals were recorded using a total number of 60 FSRs, which were embedded into four bands worn on the arm. General Regression Neural Network (GRNN) model was employed in this study for predicting the hand force in three axes from the recorded FMG signals. The regression model was trained using all possible band combinations to find the optimal placement for the FMG measurements. The results showed that the accuracy significantly improved when increasing the spatial coverage from 1 FMG band to 2 or 3 bands for all axes. While the accuracy slightly improved when the 4 bands used instead of 3. Specifically, the average R^2 across all subjects and axes are 0.68 ± 0.12, 0.84 ± 0.04, 0.91 ± 0.02 and 0.95 ± 0.01 using single, double, triple and four bands combination, respectively, in 5-fold cross-validation evaluation. The knowledge generated from this work aims serve as a guide towards the development of portable FMG based technology for widespread deployment in the general population.**

Keywords—Force Myography; Wearable sensors; Hand force estimation; Regression.

I. Introduction

Force Myography (FMG) detects the pressure exerted by the muscles toward the surface of the skin by volumetric changes induced during muscle activity [1][2]. By tracking the volumetric patterns associated with the contraction of groups of muscles, we are able to develop predictive machine learning models of gross motor function. In fact, FMG has shown a promising potential in areas of rehabilitation [3][4], prosthetic control [5][6][7], tele-operations [8], and gait analysis [9].

Although other sensor modalities, such as Electromyography (EMG), have traditionally been used to track muscle activity and motor function [10][11], FMG as measured by tactile sensors provides several advantages. Advantages of FMG are that: (1) it does not require precise sensor placement, (2) it does not require extensive skin preparation, (3) it does not require the same level of signal processing required in EMG datasets, and lastly (4) it is a more affordable alternative to other muscle activity tracking methods [12]. Moreover, it is relatively inexpensive, and easy-to-use [13]. The literature showed the usage of either EMG or FMG in regression problems for detecting grasp force [2], finger forces [14][15] and estimating the hand force/torque [16].

To measure the FMG signals, force-sensing resistors (FSRs) are employed as a row/array that can be worn around the forearm or wrist [5][17]. An FSR is a polymer thick film (PTF) which exhibits decreasing resistance with increasing applied force to the active area. As the hand exerts force, the corresponding muscles located on the arm produce deformation on the surface of the skin. These deformations apply pressure to the surface of an FSR, changing its resistance. These changes in resistance can be translated into corresponding changes in voltage that are translated into the FSRs output distinct signal patterns that can be used for hand force prediction.

Machine learning techniques have been widely employed to estimate hand force from muscular activity-based signals such as EMG and FMG, with the advantage that it does not require the knowledge about the muscle and joint dynamics [10]. Among the machine learning techniques, artificial neural network (ANN) is one of the most widely employed models due to its powerful capabilities in numerical prediction and pattern recognition [18]. In addition, ANNs are able to handle multiple classification/regression outputs by setting a number of neurons in the output layer corresponding to the target outputs; the training process (back-propagation algorithm) adjusts the weights of the network according to the training data and the true labels [19][20][21]. The regression algorithm called General Regression Neural Network (GRNN) used in this study was initially proposed by Donald F. Specht [22] in 1991. It falls into the category of probabilistic neural networks. The GRNN works as a one-pass learning algorithm with a highly parallel structure. Compared with the standard feedforward neural network such as radial basis neural network [23], GRNN has several advantages. First, GRNN is fast learning network and converges to the optimal regression surface as the number of samples becomes very large. In addition, the structure of a GRNN is relatively simple and static with 2 layers, namely pattern and summation layers [22].

The objective of this paper is to contribute to the growing understanding of the nature of FMG measurements by considering the impact of spatial coverage and sensor placement. To accomplish this, participants were invited to exert isometric force in 3 axes while wearing a custom designed portable FMG device. We hypothesize that FMG sensor placement and overall spatial coverage, with the respect to the length of the forearm, will significantly impact the accuracy and predictability of machine learning models of isometric hand force.

This paper is organized as follows: section II outlines the materials used and the proposed experimental protocol; section III provides an overview of the data processing and the regression model used; section IV presents the experimental results. Concluding remarks are presented in section V.

II. Materials and Methods

The data collection system composed of two parts. The first one is the force-sensing bands that capture the muscle contraction/expansion resulting from exerting force. The other part is the custom rig that has 6-DOF force/torque transducer that used for labeling the data.

A. Force-Sensing Band

Four customized force-sensing bands were designed to record the FMG signals from the participant's working arm. Each band utilizes 16 Force Sensitive Resistors (FSRs, Model 402 from Interlink Electronics) [24], except the wrist band which has 12 FSRs. The FSRs were housed in series into a fabric band and spaced 2 cm apart from each other. To secure the band around the participant's arm, snaps were placed on the band on either side of the FSRs. The signals from the FSRs were digitized using a voltage divider circuit with a 4.7 kΩ resistor that controls the sensitivity of the FSR and V_{DD} of 3.7 V. An ATMega328 microprocessor [25] was used to facilitate the data collection and transmission. The FSRs were sampled at 10 Hz, and the raw values were timestamped and transmitted to an on-site computer via Bluetooth connection and saved onto a .CSV file for offline processing.

Towards understanding the effect of sensor placement and spatial coverage of FMG on the arm to the hand force sensing in three axes, four bands were simultaneously donned on the participants' arm while completing a predefined protocol. The FMG bands were placed at the following 4 positions on the arm respectively: (1) approximately 2.3 cm proximal to the wrist, identified by the surface landmarks of the radial and ulnar styloid processes (2) midway between the band at position 1 and the point on the forearm with the widest circumference (3) the point on the forearm with the widest circumference, and (4) the upper arm about 2 inches above the elbow. While the widest part of the forearm is characteristically associated with the muscle bellies of intrinsic forearm's musculature, for the purpose of results reporting, this landmark be referred to as 'the muscle belly of the forearm'. The placement of these four bands used for all the participants are shown in Fig. 1.

Fig. 1. Placement of 4 customized FMG bands on participant's forearm. (1) approximately 2.25 cm proximal to the wrist, identified by the surface landmarks of the radial and ulnar styloid processes (2) midway between the band at position 1 and the point on the forearm with the widest circumference, (3) the point on the forearm with the widest circumference, and (4) on the upper arm about 2 inches above the elbow.

B. Custom Rig

A custom-built rig was designed to measure the isometric force in 3 axes denoted as F_X, F_Y, and F_Z respectively in the rest of the paper. Fig. 2 shows the setup which is composed of a base that holds a hollow plastic sphere (Fig. 2A) accommodating an ATI Mini45 6-DOF force/torque transducer [26]. The resolution of F_X, F_Y and F_Z is 1/8 N. The surface of the sphere is scratchy which prevents hand slippage during the experiments. The transducer is connected to an interface power supply box (Fig. 2B) to power it, as well as conditioning its signals to be used with a data acquisition system (Fig. 2C). The output of that interface power supply was connected to data acquisition device (DAQ) from National Instruments (NI USB 6210).

C. Software

A custom LabVIEW (© 2014) software was designed for collecting the applied force from the transducer and the FMG signals from the four bands. A visual chart showing the exerted force values was used to guide the participant to focus on one direction at a time as well as keep the sinusoidal pattern. The collected data were saved in a comma-separated values (CSV) file for offline processing and analysis.

A custom MATLAB R2015b script was designed for preprocessing the data before feeding it to the regression model to train it. Then the trained model was tested using a portion of the data that wasn't used in the training phase.

D. Participant protocol

The exerted force was collected using the 6-DOF force/torque load cell for labelling the FMG signals that were collected synchronously from four FSRs bands in different placements to explore which band(s) combination is the best for estimating each axis accurately.

Initially, the four bands were firmly and comfortably worn on specified spots on the participant's arm as on Fig. 1. Then the participant was guided to maintain the elbow angle around 90° and the shoulder angle around 45° while holding the sphere in the custom-rig to exert force on it. Each participant did the experiment for five trials. In each trial, the participant exerts isometric force in X, Y and Z directions sequentially for 40 seconds for each axis while keeping the initial position of the elbow and shoulder. The participant was guided to exert force in sinusoidal wave form for each axis to cover relatively much values. The resultant waves were visually shown on the sinusoidal pattern to help the participant to maintain the same pattern. The Data from the four bands and the 6-DOF load cell were saved in each trial.

Five healthy participants with no known neuromuscular disorder (3 females and 2 males) aged (24.2 ± 3.03 years old) participated in this study. Two anthropometric measurements of the forearm were also taken. The first measurement taken was of the forearm length, which was taken from the ulnar styloid process (bony prominence of the wrist on the side of the pinky) to the olecranon (the bony prominence of the elbow). The second measurement taken was of the circumference of the forearm at each band landmarks shown in Fig. 1. The average forearm length was 27.3 ± 1.72 cm for all five participants with circumferences of 16.2 ± 1.54 cm, 19.3 ± 2.02 cm, 24.5 ± 1.90 cm, and 25.90 ± 1.82 cm at landmarks 1, 2, 3, and 4 respectively. Subject demographics data are shown in Table I. All participants provided informed and written consent, and the test procedure was approved by the Simon Fraser University of Research Ethics.

III. Data Processing and Analysis

A MATLAB® script was designed to preprocess the data before feeding it to the regression model. The data analysis and the regression model will be described below.

A. Data Preprocessing

Initially, the readings from the sensors that were not in touch with the participant skin during the data collection were removed. The number of active sensors varied from one

TABLE I. Participant demographics

Subject	Forearm length (cm)	Circumference (cm)			
		Position 1	Position 2	Position 3	Position 4
1	26	15.5	19	25.5	27
2	25	14	16.5	22	24
3	28	15.5	18.5	23	24
4	29	18	21.5	25.5	26.5
5	28.5	17	21	26.5	28
Average (mean± STD)	27.3±1.72	16±1.54	19.3±2.02	24.5±1.9	25.9±1.82

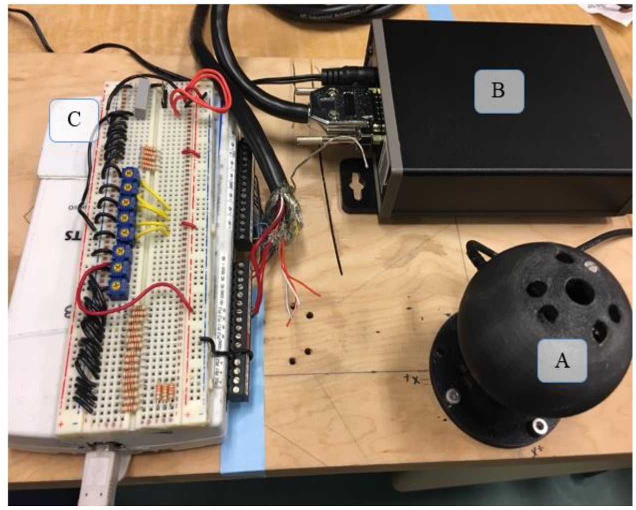

Fig. 2. The force acquisition system. (A) custom-rig used in the data collection; (B) interface power supply and (C) is the DAQ device.

participant to another based on the size of the participant's arm on each landmark as in Table I. The average number of active sensors for each band is 8, 9, 10 and 12 sensors for band 1, band 2, band 3 and band 4, respectively. After that, the active sensors readings were normalized using the global maximum and minimum values for each band. Then, the linear trend was removed from each channel of the FMG readings to eliminate the muscles fatigue effects on the signals. The linear trend line was calculated using the least-squares fit of a straight line to the FMG data and subtracting the resulting function from the data. For the true labels, a low pass Butterworth filter with a cut-off frequency of 1.5 Hz with an order selected empirically for each participant, was applied to each output of the force in three axes to remove the noise and smooth the signals.

B. Regression model

The FMG signals are corresponding to the volumetric changes on the muscles due to exerting force in any axis [2]. The literature shows the effectiveness of using the FMG signals to predict the force/torque in single axis [27] and in multi-axis [28], the objective of this paper is to explore the best placement for the FMG sensors on the arm for accurate prediction of the isometric force in 3 axes. Towards this objective, the data from all possible bands combinations was used for training a regression model then the resultant testing accuracies were compared to find the best placement(s) among the four landmarks. General Regression Neural Network (GRNN) was employed to model the FMG signals to the 3 axes force, which has a faster training speed [22].

The GRNN network consists of four layers [19]. First, the input layer has as many neurons as the number of input variables. Once the input goes through each unit in the pattern layer, the relationship between the input and the response would be memorized and stored in the unit. Thus, the number of units in the pattern layer is equal to the number of observations in the training sample. Then, the summation units perform a dot product between a weight vector and a vector composed of the signals from the pattern units. There are only two neurons in the summation layer for each output. One neuron is the denominator summation unit the other is the numerator summation unit. The denominator summation unit adds up the weight values coming from each of the hidden neurons. The numerator summation unit adds up the weight values multiplied by the actual target value for each hidden neuron as in (1). The addition of one element in the output vector requires only one summation neuron and one output neuron.

$$\hat{Y}(X) = \frac{\sum_{i=1}^{n} Y_i \exp\left[\frac{-D_i^2}{2\sigma^2}\right]}{\sum_{i=1}^{n} \exp\left[\frac{-D_i^2}{2\sigma^2}\right]} \quad (1)$$

where, $D_i^2 = (X - X_i)^T.(X - X_i)$

where X is the input sample and X_i is the training sample memorized in the unit. The output of the input sample X_i is Y_i. D_i^2 is the Euclidean distance from the X and X_i. It signifies how much the training samples can contribute to the estimate output of that particular test sample. If the distance D_i^2 is small, then the exponential in (1) will be a large value which means that the training sample will contribute more to the output prediction and vice versa. While if D_i^2 is zero, then the exponential returns one which means that the predicted output is the same as the training sample output. Finally, σ is the only unknown parameter which called spread constant. It was tuned in the training process to get the optimum value where the error is very small.

Towards comparison between different bands combinations, 5-fold cross validation was carried out with each combination where five different random permutations of the data set were generated, and then the model was trained each time on four subsets of the data set and was tested on the remaining set. To quantify the performance of the resultant model, multivariate coefficient of determination (R^2) was employed; as in (2). R^2 is a number that indicates how well the model fits the data, R^2 of 1 indicates that the model perfectly fit the data and R^2 of 0 represents that the model doesn't fit the data. Multivariate R^2 used to measure the performance of the model to predict the force in 3-DOF and it will be referred to as 3D R^2 throughout the manuscript.

$$R^2 = 1 - \frac{\sum_{i=1}^{i=D}\sum_{n=0}^{n=N}(\widehat{y_i}(n) - y_i(n))^2}{\sum_{i=1}^{i=D}\sum_{n=0}^{n=N}(y_i(n) - \overline{y_i(n)})^2} \quad (2)$$

Where D is the number of DOF that the model predicted, which is equal to 3 here, N is the number of data points, $y_i(n)$

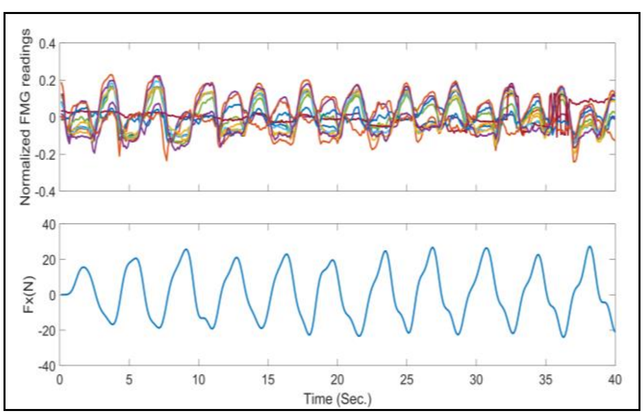

Fig. 3. An example of the normalized FMG data from band 3 and the exerted force in X direction (Fx) in N.

is the true value of the i[th] force axis, $\widehat{y_i}(n)$ is the corresponding estimate value and $\overline{y_i(n)}$ is the mean of the i[th] force axis sequence over N. Similarly, R_i^2 for individual DOF can be defined as follows:

$$R_i^2 = 1 - \frac{\sum_{n=0}^{n=N}(\widehat{y_i}(n) - y_i(n))^2}{\sum_{n=0}^{n=N}(y_i(n) - \overline{y_i(n)})^2} \quad (3)$$

IV. Results

The data was successfully collected from five participants, the total number of the collected data samples was 6000 for each participant (5 trials times 3 directions times 400 samples for focusing on each direction). Fig. 3 shows a sample of the normalized FMG data from band 3 (on the forearm muscle belly) and the force exerted in X direction for 40 seconds (one trial). It is clearly shown that both FMG signals and force have a similar pattern.

The GRNN model outputs 3 estimated values for the 3-DOF force. Table II represents the average 3D R^2 values across five subjects for the 5-fold cross-validation. It is clearly shown that increasing the spatial coverage of FMG measurements from a single FMG band to combinations of FMG bands worn on multiple arm positions resulted in significant rise in the regression accuracies. When considering FMG band placement at only 1 landmark on the arm, the results demonstrated improved accuracy when placed on the forearm muscle belly (band 3) with an average accuracy across all subjects of 0.68 ± 0.12. While using the data from other bands individually decreased the accuracy with an average of 0.12, 0.12 and 0.10 using band 1 (on the wrist), band 2 (on the forearm midway) and band 4 (on the upper arm), respectively compared to band 3 average accuracy across all subjects.

Increasing the spatial coverage of FMG measurements from single landmark to double landmarks significantly enhanced the accuracy and decreased the standard deviation. It is noticeable that all double-band combinations have comparable accuracies that ranges from 0.79 to 0.84. Overall, the combination of bands 2 and 3 show the highest average accuracy among all double-band combinations with an average of 0.84 ± 0.04.

Increasing the FMG measurements to 3 landmarks, the accuracy was much improved. Like to double-band combinations results, all triple-band combinations have similar accuracies. This could be justified in terms of increasing the number of input features, help the model to predict accurately specially for multi-output regression problems [29][30]. Both combination of bands 1, 2 and 3 and combination of bands 1, 2 and 4 achieves the highest accuracy with an average of 0.91 ± 0.02. Using all bands shows slight improvement in the accuracy with more consistent results across all subjects with an average accuracy of 0.95 ± 0.01.

Fig. 4 shows the detailed R^2 accuracy for each axis of the force in X, Y and Z. It is clearly shown that the R^2 accuracy improved for all axes with the increasing of the number of the bands used. In addition, the results become more consistent with small standard deviation when triple-band combinations or all bands used. Band 3 achieves the highest accuracy for all axes with 0.77 ± 0.07, 0.66 ± 0.12 and 0.71 ± 0.11 for F_X, F_Y, and F_Z, respectively.

While using the combination of bands 2 and 3 surged the accuracy to 0.88 ± 0.03, 0.82 ± 0.05 and 0.86 ± 0.05 for F_X, F_Y, and F_Z, respectively. Upgrading the number of bands to three, combination of bands 1, 2 and 3 achieves accuracy of 0.94 ± 0.01 0.90 ± 0.03 and 0.92 ± 0.03 for the force in X, Y and Z, respectively. Lastly, using all bands improved the accuracy to 0.96 ± 0.01, 0.94 ± 0.01 and 0.95 ± 0.01.

V. Discussion and Conclusion

The present study explored the effect of the spatial coverage and the placement of the FMG sensors on the prediction accuracy of 3 axes force. Five participants exerted isometric force in 3 axes individually while wrapping four FSRs bands around their arm on: the wrist, the forearm midway, the forearm muscle belly and the upper arm. The forces were recorded by a 6-DOF load cell to label the data. General Regression Neural Network (GRNN) was employed to train the model using all possible combinations of the four bands to find the best band(s) combination. The results showed that increasing the spatial coverage of the FMG sensors significantly improved the accuracy. In addition, the placement of the sensors contributed significantly to the prediction accuracy. For instance, when using a single band on the arm, band 3 (on the forearm muscle belly) achieves the best performance among the 4 positions, with average R^2 of 0.68 across all subjects. While using the other bands individually significantly declined the accuracy by 0.12, 0.12 and 0.10 using band 1, band 2, and band 4, respectively. This interesting finding suggests that the primary location for isometric hand force sensing should be the forearm muscle belly. In addition, it was noticeable that all the combinations that have band 3 as one of its components achieved the highest accuracy compared to the other combinations without band 3.

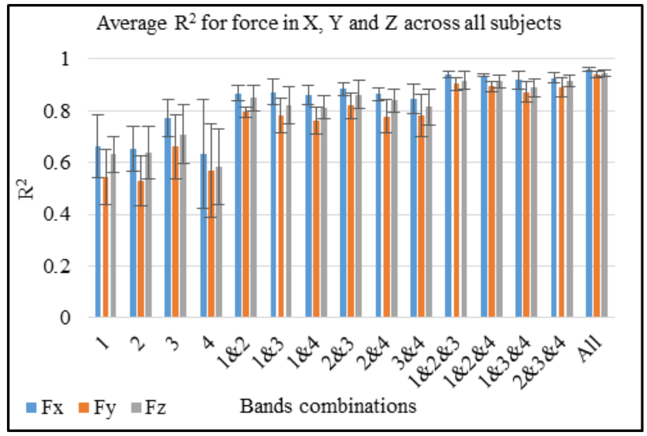

Fig. 4. The average R^2 across all subjects for the 5-fold cross validation using GRNN for the force estimated values in X, Y and Z directions.

Increasing the spatial coverage of the FMG sensors to two landmarks, improved the prediction accuracy for all axes. The R^2 improved by 0.16 when using the combination of band 2 and 3 compared to the usage of single band. This suggests for the future study to use high density FMG band that covers a large area of the forearm starting from the forearm muscle belly. While using three bands and four bands significantly improved the accuracy by 0.23 and 0.27 compared to the accuracy from using single band.

The knowledge gained from this study will provide guidance for isometric hand force estimation in terms of optimal FSR sensors placement and density on the arm.

TABLE II. 3D R^2 FROM GRNN MODELS USING ALL POSSIBLE BANDS COMBINATIONS FOR ALL SUBJECTS

	Subject 1	Subject 2	Subject 3	Subject 4	Subject 5	All Subjects
Band 1	0.36 ± 0.01	0.66 ± 0.02	0.56 ± 0.01	0.63 ± 0.003	0.59 ± 0.01	0.56 ± 0.10
Band 2	0.45 ± 0.01	0.50 ± 0.02	0.54 ± 0.01	0.67 ± 0.01	0.62 ± 0.01	0.56 ± 0.08
Band 3	0.53 ± 0.01	0.85 ± 0.01	0.66 ± 0.01	0.59 ± 0.01	0.78 ± 0.01	0.68 ± 0.12
Band 4	0.59 ± 0.02	0.74 ± 0.01	0.77 ± 0.01	0.24 ± 0.01	0.55 ± 0.01	0.58 ± 0.19
Bands 1 and 2	0.76 ± 0.01	0.85 ± 0.01	0.81 ± 0.01	0.80 ± 0.01	0.83 ± 0.01	0.81 ± 0.03
Bands 1 and 3	0.69 ± 0.01	0.90 ± 0.01	0.84 ± 0.01	0.80 ± 0.01	0.80 ± 0.01	0.81 ± 0.07
Bands 1 and 4	0.72 ± 0.01	0.87 ± 0.01	0.77 ± 0.01	0.78 ± 0.02	0.81 ± 0.01	0.79 ± 0.05
Bands 2 and 3	0.82 ± 0.01	0.92 ± 0.01	0.82 ± 0.01	0.8 ± 0.01	0.82 ± 0.004	0.84 ± 0.04
Bands 2 and 4	0.82 ± 0.01	0.87 ± 0.01	0.74 ± 0.01	0.79 ± 0.01	0.80 ± 0.01	0.80 ± 0.04
Bands 3 and 4	0.69 ± 0.01	0.93 ± 0.004	0.78 ± 0.003	0.75 ± 0.01	0.82 ± 0.01	0.79 ± 0.08
Bands 1, 2 and3	0.92 ± 0.01	0.95 ± 0.004	0.92 ± 0.01	0.88 ± 0.01	0.91 ± 0.01	0.91 ± 0.02
Bands 1, 2 and 4	0.91 ± 0.002	0.93 ± 0.01	0.89 ± 0.01	0.89 ± 0.01	0.92 ± 0.04	0.91 ± 0.02
Bands 1, 3 and 4	0.80 ± 0.01	0.93 ± 0.01	0.90 ± 0.004	0.89 ± 0.01	0.89 ± 0.01	0.88 ± 0.04
Bands 2, 3 and 4	0.90 ± 0.004	0.95 ± 0.002	0.89 ± 0.01	0.90 ± 0.01	0.88 ± 0.01	0.90 ± 0.03
Bands 1, 2, 3 and 4	0.95 ± 0.003	0.96 ± 0.002	0.95 ± 0.01	0.94 ± 0.01	0.94 ± 0.001	0.95 ± 0.01

Acknowledgment

This research was supported by the Natural Sciences and Engineering Research Council of Canada (NSERC), the Canadian Institutes of Health Research (CIHR), and the Michael Smith Foundation for Health Research (MSFHR).

References

[1] S. L. Phillips and W. Craelius, "Residual kinetic imaging: a versatile interface for prosthetic control," *Robotica*, vol. 23, no. 3, pp. 277–282, 2005.

[2] M. Wininger, N.-H. Kim, and W. Craelius, "Pressure signature of forearm as predictor of grip force.," *J. Rehabil. Res. Dev.*, vol. 45, no. 6, pp. 883–892, Jan. 2008.

[3] G. Sadarangani and C. Menon, "Gautam Sadarangani, Carlo Menon, Member, IEEE," pp. 672–677, 2015.

[4] G. Sadarangani and C. Menon, "A wearable sensor system for rehabilitation apllications," in *2015 IEEE International Conference on Rehabilitation Robotics (ICORR)*, 2015, pp. 672–677.

[5] M. Connan, E. Ruiz Ramírez, B. Vodermayer, and C. Castellini, "Assessment of a Wearable Force- and Electromyography Device and Comparison of the Related Signals for Myocontrol," *Front. Neurorobot.*, vol. 10, no. November, pp. 1–13, 2016.

[6] E. R. Ramírez, "Control of a hand prosthesis using mixed electromyography and pressure sensing," 2016.

[7] C. Castellini, P. Artemiadis, M. Wininger, A. Ajoudani, M. Alimusaj, A. Bicchi, B. Caputo, W. Craelius, S. Dosen, K. Englehart, D. Farina, A. Gijsberts, S. B. Godfrey, L. Hargrove, M. Ison, T. Kuiken, M. Markovi??, P. M. Pilarski, R. Rupp, and E. Scheme, "Proceedings of the first workshop on peripheral machine interfaces: Going beyond traditional surface electromyography," *Front. Neurorobot.*, vol. 8, no. AUG, p. 22, Aug. 2014.

[8] R. Khurshid, N. Fitter, E. Fedalei, and K. Kuchenbecker, "Effects of Grip-Force, Contact, and Acceleration Feedback on a Teleoperated Pick-and-Place Task," *IEEE Trans. Haptics*, 2016.

[9] D. A. Yungher, M. T. Wininger, J. B. Barr, W. Craelius, and A. J. Threlkeld, "Surface muscle pressure as a measure of active and passive behavior of muscles during gait," *Med. Eng. Phys.*, vol. 33, no. 4, pp. 464–471, May 2011.

[10] D. Yang, J. Zhao, Y. Gu, L. Jiang, and H. Liu, "Estimation of hand grasp force based on forearm surface EMG," *Mechatronics and Automation, 2009. ICMA 2009. International Conference on*. pp. 1795–1799, 2009.

[11] F. Mobasser and K. Hashtrudi-Zaad, "Hand force estimation using electromyography signals," in *Proceedings of the 2005 IEEE International Conference on Robotics and Automation*, 2005, pp. 2631–2636.

[12] V. Ravindra and C. Castellini, "A Comparative Analysis of Three Non-Invasive Human-Machine Interfaces for the Disabled," *Front. Neurorobot.*, vol. 8, no. October, pp. 1–10, 2014.

[13] C. Castellini and V. Ravindra, "A wearable low-cost device based upon Force-Sensing Resistors to detect single-finger forces," in *5th IEEE RAS/EMBS International Conference on Biomedical Robotics and Biomechatronics*, 2014, pp. 199–203.

[14] V. Ravindra and C. Castellini, "A Comparative Analysis of Three Non-Invasive Human-Machine Interfaces for the Disabled," *Front. Neurorobot.*, vol. 8, p. 24, Oct. 2014.

[15] R. L. Abboudi, C. A. Glass, N. A. Newby, J. A. Flint, and W. Craelius, "A biomimetic controller for a multifinger prosthesis," *IEEE Trans. Rehabil. Eng.*, vol. 7, no. 2, pp. 121–129, Jun. 1999.

[16] M. Ison, I. Vujaklija, B. Whitsell, D. Farina, and P. Artemiadis, "High-density electromyography and motor skill learning for robust long-term control of a 7-DoF robot arm," *IEEE Trans. Neural Syst. Rehabil. Eng.*, vol. 24, no. 4, pp. 424–433, 2016.

[17] A. Dementyev and J. A. Paradiso, "WristFlex: Low-Power Gesture Input with Wrist-Worn Pressure Sensors," in *Proceedings of the 27th annual ACM symposium on User interface software and technology - UIST '14*, 2014, pp. 161–166.

[18] B. Yegnanarayana, *Artificial neural networks*. PHI Learning Pvt. Ltd., 2009.

[19] J.-J. Luh, G.-C. Chang, C.-K. Cheng, J.-S. Lai, and T.-S. Kuo, "Isokinetic elbow joint torques estimation from surface EMG and joint kinematic data: using an artificial neural network model," *J. Electromyogr. Kinesiol.*, vol. 9, no. 3, pp. 173–183, 1999.

[20] E. N. Kamavuako, E. J. Scheme, and K. B. Englehart, "Wrist torque estimation during simultaneous and continuously changing movements: surface vs. untargeted intramuscular EMG," *J. Neurophysiol.*, vol. 109, no. 11, pp. 2658–2665, 2013.

[21] M. H. Shahmoradi, M. A. Akhaee, and M. S. Mirian, "Combined classification and regression for simultaneous and proportional EMG control of wrist forces," in *Signal Processing Conference (EUSIPCO), 2015 23rd European*, 2015, pp. 2426–2430.

[22] D. F. Specht, "A general regression neural network," *IEEE Trans. neural networks*, vol. 2, no. 6, pp. 568–576, 1991.

[23] H. B. Demuth, M. H. Beale, O. De Jess, and M. T. Hagan, *Neural Network Design*, 2nd ed. USA: Martin Hagan, 2014.

[24] InterlinkElectronics, "FSR® Integration Guide & Evaluation Parts Catalog with Suggested Electrical Interfaces," 2010.

[25] Atmel Corporation, "ATmega328 / P Datasheet," p. 24, 2016.

[26] A. I. Automation, "F/T Sensor Mini45," 2015. [Online]. Available: http://www.ati-ia.com/app_content/documents/9620-05-DAQ.pdf. [Accessed: 01-Sep-2015].

[27] M. Sakr and C. Menon, "Regressing force-myographic signals collected by an armband to estimate torque exerted by the wrist: A preliminary investigation," in *2016 IEEE Canadian Conference on Electrical and Computer Engineering (CCECE)*, 2016, pp. 1–4.

[28] M. Sakr and C. Menon, "On the estimation of isometric wrist/forearm torque about three axes using Force Myography," in *Biomedical Robotics and Biomechatronics (BioRob), 2016 6th IEEE International Conference on*, 2016, pp. 827–832.

[29] C. Bishop and N. Nasrabadi, "Pattern recognition and machine learning," *COMPSTAT*, pp. 325–358, 2006.

[30] H. Borchani, G. Varando, C. Bielza, and P. Larranaga, "A survey on multi-output regression," *Wiley Interdiscip. Rev. Data Min. Knowl. Discov.*, vol. 5, no. 5, pp. 216–233, 2015.